Insect Biochemistry and Molecular Biology 43 (2013) 336–343

Contents lists available at SciVerse ScienceDirect

Insect Biochemistry and Molecular Biology

journal homepage: www.elsevier.com/locate/ibmb

Functional characterization of myrcene hydroxylases from two geographically distinct *Ips pini* populations

Minmin Song [a], Amy C. Kim [a], Andrew J. Gorzalski [a], Marina MacLean [a], Sharon Young [a], Matthew D. Ginzel [b], Gary J. Blomquist [a], Claus Tittiger [a,*]

[a] Department of Biochemistry and Molecular Biology, University of Nevada, Reno, NV 89557, USA
[b] Departments of Entomology and Forestry and Natural Resources, Purdue University, West Lafayette, IN 47907, USA

ARTICLE INFO

Article history:
Received 12 July 2012
Received in revised form
7 January 2013
Accepted 15 January 2013

Keywords:
Cytochrome P450
Monoterpene
Pheromone
Detoxification
Functional assay

ABSTRACT

Ips pini bark beetles use myrcene hydroxylases to produce the aggregation pheromone component, ipsdienol, from myrcene. The enantiomeric ratio of pheromonal ipsdienol is an important prezygotic mating isolation mechanism of *I. pini* and differs among geographically distinct populations. We explored the substrate and product ranges of myrcene hydroxylases (*CYP9T2* and *CYP9T3*) from reproductively-isolated western and eastern *I. pini*. The two cytochromes P450 share 94% amino acid identity. *CYP9T2* mRNA levels were not induced in adults exposed to myrcene-saturated atmosphere. Functional assays of recombinant enzymes showed both hydroxylated myrcene, (+)- and (−)-α-pinene, 3-carene, and *R*-(+)-limonene, but not α-phellandrene, (−)-β-pinene, γ-terpinene, or terpinolene, with evidence that *CYP9T2* strongly preferred myrcene over other substrates. They differed in the enantiomeric ratios of ipsdienol produced from myrcene, and in the products resulting from different α-pinene enantiomers. These data provide new information regarding bark beetle pheromone evolution and factors affecting cytochrome P450 structure–function relationships.

1. Introduction

The pine engraver, *Ips pini* (Say) (Coleoptera: Scolytinae), is broadly distributed across North America, infesting a variety of weakened or recently dead pines, often after a host has previously been compromised by the mountain pine beetle (*Dendroctonus ponderosae*). The major pine engraver aggregation pheromone component is ipsdienol (2-methyl-6-methylene-2,7-octadien-4-ol), produced *de novo* via the mevalonate pathway in anterior midguts of pioneer males (rev. Blomquist et al., 2010). The enantiomeric composition of ipsdienol is functionally important: western populations use >95% (−)-ipsdienol as a pheromone, whereas eastern populations produce and respond to an approximately 60:40 ratio of (−)-:(+)-ipsdienol. The difference is attributed to one or a few loci (Domingue and Teale, 2008). Thus, eastern and western populations are reproductively isolated both by geography and by their indifference to the other's aggregation pheromone, although individuals from each population can produce fertile offspring in no-choice mating experiments (Domingue et al., 2006).

These geographically-distinct populations provide an opportunity to study how pheromone systems evolve at a molecular and biochemical level. Of particular interest are cytochromes P450 because of their importance in both endogenous metabolism and xenobiotic clearing (Feyereisen, 2005). However, while many studies report expression data in the context of environmental challenges, surprisingly few insect P450s have been functionally characterized. Indeed, pioneering efforts to map papilionid butterfly substrate ranges showed that substrate profiles of closely-related detoxifying P450 orthologs correlate with host ranges, and illustrate the utility of biochemical characterization in understanding the molecular mechanisms contributing to host range evolution (Li et al., 2003; Mao et al., 2006; Wen et al., 2003). These studies are thus useful to understand both insect evolution and P450 enzymology.

In western *I. pini*, *CYP9T2* encodes a cytochrome P450 that hydroxylates myrcene to produce ipsdienol. It is coordinately regulated with other pheromone-biosynthetic enzymes and appears to function solely in pheromone biosynthesis (Sandstrom et al., 2006). However, the substrate range for *CYP9T2* has not been determined. *CYP9T2* produces ~80:20 (−)-:(+)-ipsdienol; and this intermediate product is further acted upon by at least one other enzyme (ipsdienol dehydrogenase, (Figueroa-Teran et al., 2012) to "tune" the enantiomeric ratio toward the pheromonal blend. Here, we further

* Corresponding author.
E-mail address: crt@unr.edu (C. Tittiger).

0965-1748/$ – see front matter © 2013 Elsevier Ltd. All rights reserved.
http://dx.doi.org/10.1016/j.ibmb.2013.01.003

characterize *CYP9T2* from a western population, introduce a novel myrcene hydroxylase, *CYP9T3*, from an eastern population, and compare their substrate and product profiles.

2. Materials and methods

2.1. Reagents and chemicals

Hink's 1X TNM-FH Medium (Supplemented Grace's Medium) and Grace's 1X Insect Basal Medium were from Mediatech, Inc. (Herndon, VA) and FBS was from Atlas Biologicals (Fort Collins, CO). The housefly cytochrome P450 reductase baculoviral clone (Wen et al., 2003) was kindly provided by M. Schuler (U. Illinois at Urbana-Champaign). Agarose was from ISC Bioexpress (Keysville, UT). Phenylmethylsulfonyl fluoride (PMSF), (+)- and (−)-α-pinene (81% e.e.), Δ3-carene, α-phellandrene, β-pinene, γ-terpinene, myrcene, terpinolene, *R*-(+)- limonene, *cis*-verbenol, protease inhibitor cocktail, δ-aminolevulinic acid and ferric citrate were from Sigma–Aldrich (St. Louis, MO). Ipsdienol and *trans*-verbenol standards were from Contech Inc. (Victoria, BC). UV Star 96-well microplates were from Greiner Bio-One (Monroe, North Carolina). The ReadiUse™ NADPH Regenerating Kit was from AAT Bioquest (Sunnyvale, CA). Primers for PCR and sequencing were purchased from Sigma–Aldrich or IDT Technologies, and are listed in Supplementary Table 1.

2.2. Insects

Immature *I. pini* from a western population (w*Ip*) were obtained from infested Jeffrey pine (*Pinus jeffreyi*) bolts collected from Little Valley (39°15′00 N′, 119°52′30 W), allowed to mature, and collected as per (Browne, 1972). Individuals were separated by sex and stored on moist paper towels at 4 °C for no longer than two weeks prior to use. For the myrcene-exposure experiment, groups of five males or females/sample were placed in glass-stoppered bottles with a piece of Whatman filter paper containing four μl myrcene and incubated in a humidified chamber (to prevent desiccation) in the dark for 20 h. Control groups were treated identically, except that water was used instead of myrcene. Following incubation, midguts were dissected from beetles submerged in distilled water and then frozen at −80 °C until RNA extraction. There were three samples for female beetles, and four for males.

Eastern *I. pini* (*eIp*) were reared from infested white pine (*Pinus strobus*) collected at Martell Forest (40°26′12″N, 87°1′53″W) in Tippecanoe Co., IN. Males were placed in small holes drilled into the phloem of Jeffrey pine (*Pinus jeffreyi*) bolts, secured with wire mesh, and allowed to feed for 24 h. Anterior midguts from five individuals were then removed, pooled, and stored at −80 °C until RNA was extracted using an RNeasy Plant Mini Kit (Qiagen). First strand cDNA was produced from the RNA bed with SuperScript III reverse transcriptase and T_{17}CSX primer as per the manufacturer's protocol (Life Technologies).

2.3. CYP9T2 expression analysis

Total RNA was extracted from midguts using the RNeasy Plant Mini Kit as per the manufacturer's protocol (Qiagen) and reverse transcribed using Superscript III (Stratagene) and random hexamer primers (Invitrogen) essentially as per (Sandstrom et al., 2006). Primers for quantitative (Real Time)-reverse transcriptase PCR (qRT-PCR) of *cytoplasmic actin* and *CYP9T2* were as per (Keeling et al., 2006). Primers for qRT-PCR amplification of *GAPDH* and *Ubiquitin* were designed from EST sequences (Keeling et al., 2006) using Primer Express software (Applied Biosystems), screened for potential primer-dimer and hairpin loop formation with Vector NTI Advance 9 (Invitrogen), and selected as appropriate housekeeping genes using GeNorm software (Hellemans et al., 2007). Selected primer sets were tested for non-specific amplification by visual inspection of melting curves. Reaction plates contained 7.5 μl template, 0.3 μM each primer, and 12.5 μl SYBR Green master mix (Eurogentec) in 25 μl, total. The samples were analyzed on an ABI PRISM 7000 Sequence Detection System at the Nevada Genomics Center. Relative expression values for *CYP9T2* and *GPPS/MS* (Gilg et al., 2005) normalized to *cytoplasmic actin*, *GAPDH*, and *Ubiquitin* were calculated using qBase software (Hellemans et al., 2007).

2.4. CYP9T3 functional cloning

CYP9T2 sequence-specific primers were used to obtain a full length clone of *CYP9T2* from e*Ip* cDNA. Various clones were sequenced with an ABI3730 DNA Analyzer at the Nevada Genomics Center and analyzed with Vector NTIv.9 software (Informax, N. Bethesda, MD) and CLC Workbench v. 6.7.1. The *CYP9T3* clone was chosen for further study because its sequence was most dissimilar to *CYP9T2*. The full length *CYP9T3* ORF was amplified by PCR using forward and reverse primers designed using Clontech's online tool, directionally cloned into pENTR-*Nco*I (Sandstrom et al., 2006) using an InFusion®HD Cloning Kit (Clontech), and transformed into Stellar™ Competent Cells (Clontech). Fifty uL PCR reactions contained 25 pmol each forward and reverse primers, 0.2 mM dNTPs, 1X *PfuUltra* II Reaction Buffer, and *PfuUltra* II Fusion HS DNA Polymerase (Agilent, La Jolla, CA). Cycling parameters for the linker ramp profile were: 95 °C for 1 min, three cycles of 94 °C for 40 s, 65 °C for 1 min, 0.3 °C/s to 72 °C, and 72 °C for 45 s followed by 35 cycles of 94 °C for 40 s, 65 °C for 30 s, 72 °C for 45 s ending with a final extension at 72 °C for 2 min. The recombinant plasmid, pENTR-*NcoI_CYP9T3*, was confirmed by sequencing, transferred into BaculoDirect (Invitrogen) baculoviral expression vector by an LR recombinase reaction (Invitrogen) and used to infect Sf9 cells in the presence of ganciclovir to select for recombinant virus. High titer P3 viral stocks for each construct were produced by successive 72 h–120 h amplifications of the initial and P2 viral stocks. *CYP9T3* recombinant baculoviral stock was confirmed with PCR. An approximate viral titer was determined by a plaque assay.

2.5. Recombinant protein production

Protocols for growth and maintenance of Sf9 cells and heterologous expression using the BaculoDirect™ Expression System were as described by Invitrogen. δ-Aminolevulinic acid (0.3 mM final conc.) and ferric citrate (0.2 mM final conc.) were added at the time of infection. To produce recombinant *CYP9T2* or housefly cytochrome P450 reductase (CPR; Wen et al., 2003), Sf9 cells were infected with recombinant baculovirus at multiplicities of infection (MOI) = 0.4 for *CYP9T2*, and 0.1 for CPR as described previously (Sandstrom et al., 2006). Co-expression of *CYP9T3* and HF-CPR was performed by co-infecting Sf9 cells with *CYP9T3* and CPR viral stocks at MOIs 0.4 and 0.1, respectively. Sf9 cells were cultured at 27 °C with shaking flask and all samples were harvested on day 3 post-infection (PI).

2.6. Microsome preparation

Sf9 cells and Sf9 cells producing recombinant *CYP9T2*, CPR, or *CYP9T3* and CPR were harvested at day 3 PI, and microsomes were prepared by differential centrifugation essentially as per (Wen et al., 2003). Briefly, cells were pelleted by centrifugation at 3000 × g at 4 °C for 10 min. The pellets were resuspended in 1/5 cell culture volume of 100 mM ice-cold sodium phosphate buffer (pH 7.8) and repelleted twice at 3000 × g for 10 min. The pellets were

resuspended in 1/30 cell culture volume of ice-cold cell lysate buffer (100 mM sodium phosphate pH 7.8, 1.1 mM EDTA, 0.1 mM DTT, 0.5 mM PMSF, 1/1000 vol/vol Sigma protease inhibitor cocktail, 20% glycerol) and lysed by sonication three times for 15 s on ice with a Branson Sonifier 450, followed by vortexing for 15 s. The lysate was centrifuged at 10,000 × g for 20 min at 4 °C in a microcentrifuge and the supernatant was further centrifuged in a TLA-110 rotor at 120,000 × g for 2 h in a Beckman–Coulter Optima ultracentrifuge to pellet microsomes. The microsomal pellet was resuspended in 1/30 cell culture volume of ice-cold cell lysate buffer and used immediately.

2.7. CO-Difference microplate assay

Functional P450 concentrations in microsomes containing recombinant *CYP9T2* or CYP09T3 were determined by CO-difference spectrum analysis (Omura and Sato, 1964) using a 96-well microplate and SpectraMax M5 Microplate Reader coupled with SoftMax® Pro software (Molecular Devices, Inc., Sunnyvale, CA) essentially as per (Choi et al., 2003). Briefly, 200 μl or 100 μl of microsome solution from each group was loaded into replicate wells for reference and CO treatment samples. The reference wells were tightly sealed with cellophane tape, and the plate was placed in a plastic chamber. CO gas was perfused into the top of the chamber and out from the bottom at 0.5 l/min for 3 min. All samples were reduced by adding fresh 0.5 M sodium hydrosulfite to 25 mM. The absorbances from 400 to 500 nm were measured with a SpectraMax M5 Microplate Reader. The P450 concentration was calculated using the following formula:

$$[P450](mM) = \chi^{*}(\mathbf{\Delta}450 - \mathbf{\Delta}490)/91 \quad (1)$$

where Δ450 and Δ490 are the absorbance differences between the CO sample and reference sample at 450 nm and 490 nm respectively, and χ represents the conversion factor for the molar extinction coefficient (1.9 or 3.8 for 200 μl or 100 μl respectively in a 6.96 mm diameter well relative to a 1 cm light pathway). The total protein concentration in each microsomal sample was quantified using the Pierce BCA Protein Assay Kit as recommended by the supplier (Thermo Scientific, Rockford, IL).

2.8. Enzyme assays

Enzyme assays were conducted in 500 μl reactions containing 468 μl or 250 μl of a 4:1 mixture of microsomes bearing recombinant *CYP9T2* or CPR or microsomes bearing both recombinant *CYP9T3* and CPR, 200–300 μM monoterpene in pentane, and 300 μM NADPH or 250 μl 2X NADPH regenerating system. Reactions were initiated with the addition of NADPH or NADPH regeneration system, incubated in a 30 °C water bath for 30 min to 6 h, and then extracted twice with pentane:ether (1:1) spiked with 5–250 μg/ml *n*-octanol (internal standard). The organic phase was concentrated to approximately 50–100 μl with N_2 gas and directly analyzed by coupled GC–MS at the Nevada Proteomics Center (UNR). Negative controls reactions were performed as above with microsomes prepared from cells infected with recombinant CPR baculovirus only. A Thermo Finnigan Polaris Q ion trap was used with a molecular weight scanning range of 40–180 atomic mass unit (amu) at an ionization potential of 70 eV. A trace gas chromatograph containing a 60 m × 0.25 mm (ID), 0.25 μm film thickness DB-5 capillary column (J&W Scientific, Palo Alto, CA) was programmed for an initial temperature of 50 °C (1 min hold), increase to 200 °C at 5 °C/min, 10 °C/min to 320 °C (20 min hold). The injector was split at a ratio of 100:1 at a temperature of 280 °C with a column flow of 1.5 ml He/min. The detector was set at 200 °C. The product was identified by comparing retention times and mass spectra with negative controls and authentic standards.

Recombinant *CYP9T2* co-expressed with HF-CPR was assayed with 250 μM myrcene using the same protocol as above. The enantiomeric composition of ipsdienol produced from assays of myrcene incubated for 2 h with either CYP9T2-CPR or CYP9T3-CPR were determined by chiral separation using the same GC–MS with a CycloSil-B (30 m × 0.25 mm internal diameter, 0.25 μm film thickness) column (J&W Scientific) that was isothermal at 100 °C for 45 min and a flow rate of 1.3 ml He/min. Products were identified by comparing retention times and mass spectra to those of authentic standards. Relative amounts of (4*R*)-(−)-ipsdienol and (4*S*)-(+)-ipsdienol were determined by dividing the integrated area of each corresponding peak by the sum of the integrated areas of both peaks.

For the competition experiments, 0.5 ml reactions contained a mixture of 126 μM (+)-α-pinene and 116 μM myrcene or 128 μM 3-carene and 116 μM myrcene (final concentrations), and a 4:1 (v:v) mixture of microsomes bearing recombinant *CYP9T2* and CPR. The 2X NADPH regeneration system was added to initiate the reactions. The enzyme assays were incubated in a 30 °C water bath for 3 h and extracted as described above. Sf9 cell microsomes bearing CPR were used as a negative control. Extracts were analyzed using a Shimadzu GC fitted with an HP-INNOWax column (Agilent) programmed for an initial temperature of 40 °C, increase to 240 °C at 4 °C/min, hold for 5 min. The detector was set at 260 °C. The percentage of substrate conversion was calculated according to areas of product and substrate by dividing the amount of product by the total amount of products and substrates.

3. Results

3.1. CYP9T3 sequence

Probing eastern *I. pini* (e*Ip*) fed male anterior midgut cDNA for CYP9T2-related sequences revealed a 1598 nt sequence containing a 1598 nt open reading frame (ORF) (Supplementary Figure 1). The cDNA was completely sequenced (GenBank I.D. KC437379) and designated *CYP9T3* by the P450 nomenclature committee (http://drnelson.uthsc.edu/CytochromeP450.html). The ORF encodes a 532 amino acid (a.a.) protein with a mass of 61 kDa and pI of ~8.97 (CLC Workbench v. 6.7.1). The deduced amino acid sequence has many conserved P450 domains including WxxxR, ExxR, and PxxFxPERF motifs and a heme-binding domain (PFxxGxRxCxG) (Fig. 1). The predicted translation product had 94% identity and 98% similarity with the western *I. pini* (w*Ip*) myrcene hydroxylase, *CYP9T2* (Sandstrom et al., 2006) (Fig. 1). A BLAST (Altschul et al., 1990) search shows *CYP9T3* is 95% identical to *Ips confusus* CYP9T1 (GenBank i.d. ACK37844.1; Sandstrom et al., 2008), 96% identical to *Ips paraconfusus* CYP9T1 (ABF06554.1; Huber et al., 2007), and 44% identical ($E = 3e\text{-}163$) to *Dendroctonus ponderosae* CYP9Z18 (AFI45045).

3.2. mRNA profiles

Myrcene hydroxylase (*CYP9T2*) and geranyl diphosphate synthase/myrcene synthase (*GPPS/MS*) were more highly expressed in male midguts compared to female midguts of unfed beetles that were exposed to a myrcene-saturated atmosphere for 20 h (Fig. 2). However, myrcene exposure did not significantly change either gene's expression level (Student's *T*-Test, $p < 0.21$ and 0.18 for *CYP9T2* and *GPPS/MS* in female tissues, and $p < 0.17$ and 0.43 for *CYP9T2* and *GPPS/MS* in male tissues, respectively).

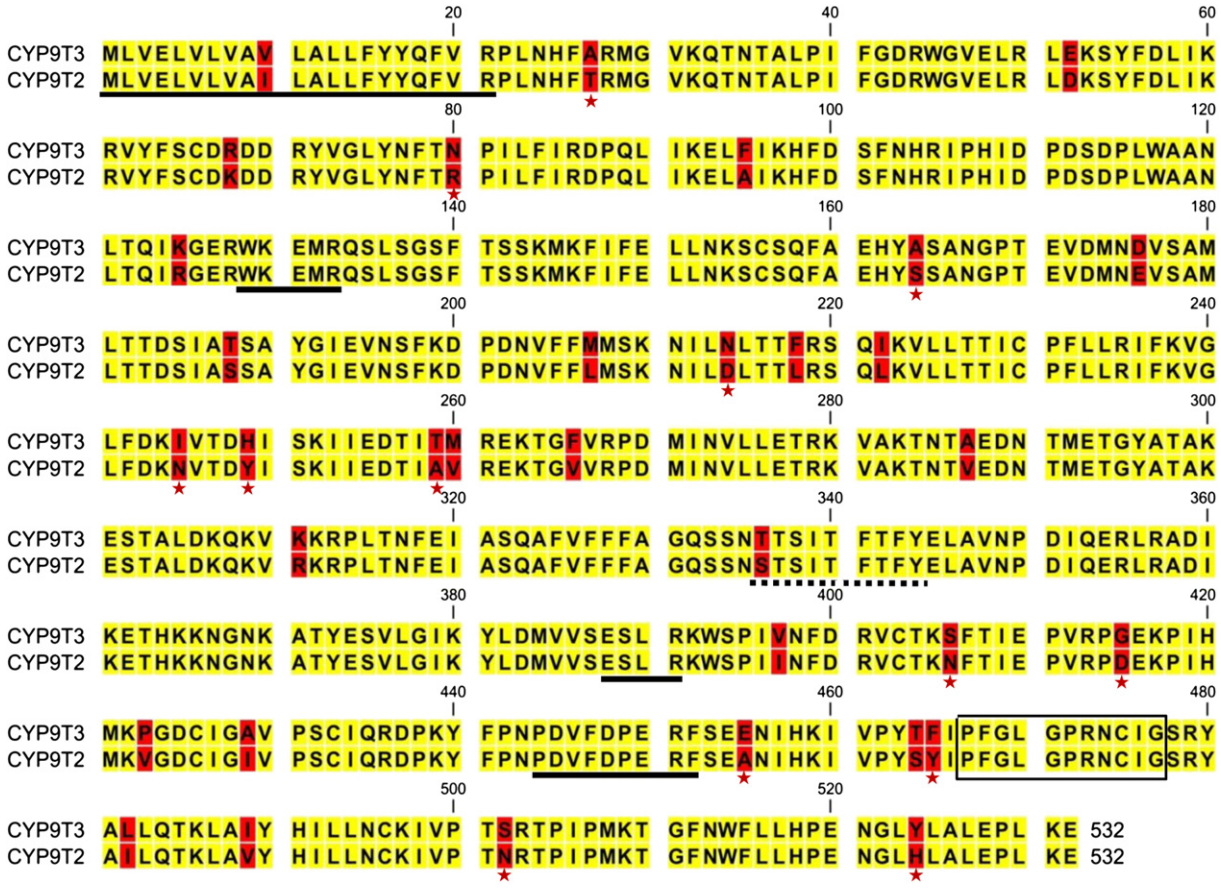

Fig. 1. Alignment of *CYP9T2* and *CYP9T3*. Identical and similar amino acids are highlighted yellow and red, respectively. Non-conserved positions have a red star below the alignment. The N-terminal membrane anchor sequence and conserved WxxxR, ExxR, and PxxFxPERF motifs, solid underline; predicted membrane associated sequence, dashed underline. The heme-binding domain (PFxxGxRxCxG) is boxed. SRS – substrate recognition site.

3.3. Ipsdienol enantiomeric ratios

In order to determine the enantiomeric ratio of ipsdienol produced from myrcene by *CYP9T2* and *CYP9T3*, products were separated on a Cyclosil-B (chiral) column. Each incubation yielded two products with the same elution times and mass spectra as (−)- and (+)-ipsdienol (Fig. 3A). The enantiomeric ratio of 88.7% (4*R*)-(−):11.3% (4*S*)-(+)-ipsdienol produced by *CYP9T3* was significantly different than the 81.0% (4R)-(−):19.0%(−)-ipsdienol ratio seen with *CYP9T2* (Fig. 3B) ($p < 0.00025$ Student's *t*-test, $n = 4$).

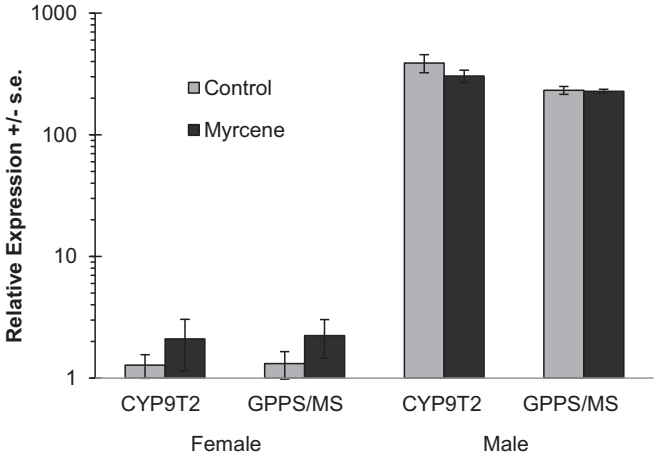

Fig. 2. Relative *CYP9T2* and GPPS/MS mRNA levels in midguts of unfed *I. pini* that were exposed to myrcene vapors for 20 h (Myrcene). Values (means ± std. err.) were determined by qRT-PCR, normalized to those for the housekeeping genes *cytoplasmic actin*, *GAPDH*, and *Ubiquitin*, and are relative to those for the female control samples, which were set at one.

3.4. Substrate range assays

Recombinant *CYP9T2* and *CYP9T3* were assayed for the ability to hydroxylate various monoterpenes *in vitro*. Substrates and products are listed in Table 1. GC–MS analyses of pentane:ether extracts showed no detectable products for either enzyme in assays with α-phellandrene, (−)-β-pinene, γ-terpinene, or terpinolene (not shown). Assays incubated with myrcene yielded exclusively ipsdienol (Fig. 3 and not shown). Assays incubated with (+)- and (−)-α-pinene yielded products with retention times and mass spectra identical to those for *trans*-verbenol and myrtenol, respectively for *CYP9T2*, The products appeared to be stereo-specific, as no myrtenol was detected in incubations with (+)-α-pinene, and no verbenols were detected in incubations with (−)-α-pinene (Fig. 4A, C). Similarly, assays with *CYP9T3* produced *cis*- and *trans*-verbenol, respectively, from (+)- and (−)-α-pinene (Fig. 4B, D).

Assays with 3-carene yielded single products from each enzyme, each with a similar mass spectrum – the only difference being the presence of an 81.1 *m*/*z* peak for the *CYP9T2* product, whereas the product from the *CYP9T3* reaction produced a 79.0 *m*/*z* peak (Fig. 5, A, B). When assayed with (*R*)-(+)-limonene, both enzymes produced a single product with essentially identical mass spectra

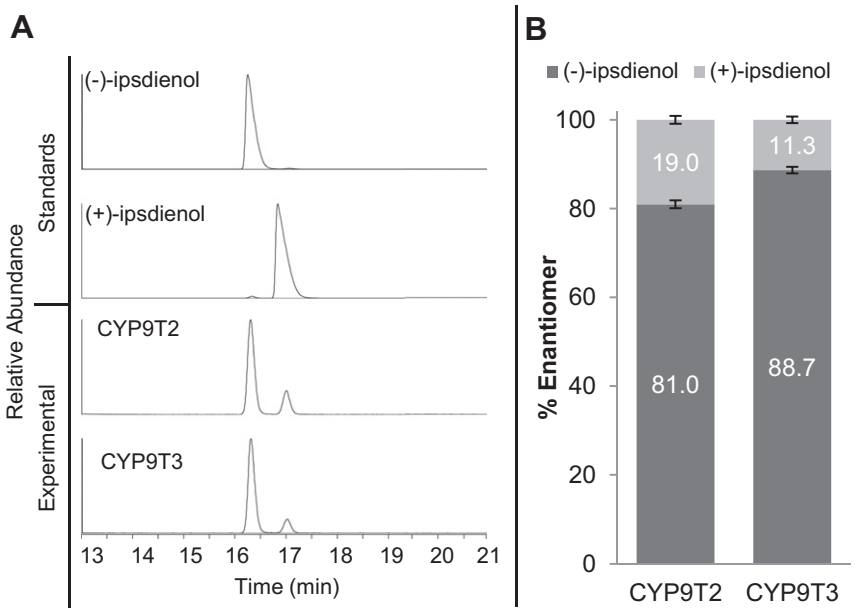

Fig. 3. Enantiomeric ratios of (−)- and (+)-ipsdienol produced from myrcene by recombinant *CYP9T3* or *CYP9T2* co-expressed with CPR. (**A**) Representative GC traces from a CycloSil-B (chiral) column (Boxcar smoothing, 7 points applied) showing (−)-ipsdienol at 16.4 min and (+)-ipsdienol at 17.1 min. (**B**) Comparison of the ratio of (−)-ipsdienol to (+)-ipsdienol as produced by *CYP9T2*:CPR and *CYP9T3*:CPR based on GC–MS analysis ($m/z = 85$) of peaks in **A**. Values are means ± std. dev., $n = 4$, $p < 0.00025$ (Student's *t*-test).

(Fig. 5C, D). The mass spectra of products from 3-carene and limonene were different, but consistent with hydroxylated monoterpenes; neither matched conclusively with spectra from known standards (not shown). No monoterpenoid alcohol products were observed in negative control reactions, except for small peaks corresponding to verbenol that were occasionally observed in incubations with recombinant CPR (not shown).

3.5. Substrate competition assays

To test *CYP9T2* substrate preferences, enzyme assays were performed with the mixture of (+)-α-pinene and myrcene or 3-carene and myrcene. For 3 h incubations, reactions containing the mixture of (+)-α-pinene and myrcene converted approximately 13% (+)-α-pinene to verbenol and about 46% myrcene to ipsdienol, while given a mixture of 3-carene and myrcene, about 10% of the 3-carene was converted to an unknown product and 48% of the myrcene was hydroxylated to ipsdienol (Fig. 6). Longer incubation times (6 h) yielded higher amounts (not shown). Negative controls with recombinant CPR did not yield these products (Fig. 6 and not shown).

4. Discussion

Geographically distinct *I. pini* populations produce and respond to different blends of (*R*)-(−)- and (*S*)-(+)-ipsdienol. *CYP9T3* cDNA was isolated from an "eastern" *I. pini* population in Indiana. Although there is a hybrid zone near the Rocky Mountains, western and eastern populations display assortative mating (Hager and Teale, 1996) and there is apparent pressure to maintain variation in pheromone blends (Shumate et al., 2011). While it was initially proposed that myrcene hydroxylases produce the correct enantiomeric ratio because of their role in pheromone biosynthesis, it is now clear that they do not (Sandstrom et al., 2008). Nevertheless, mapping myrcene hydroxylase substrate and product profiles is useful because the information gained can help to understand both

Table 1
CYP9T2 and *CYP9T3* substrate and product profiles.

Substrate[a]		Product			
		CYP9T2		*CYP9T3*	
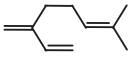	Myrcene		Ipsdienol [80:20 (−):(+)]		Ipsdienol [87:13 (−):(+)]
	(+)-α-pinene		Verbenol		Verbenol
	(−)-α-pinene	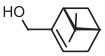	Myrtenol		*cis*-verbenol
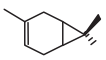	3-carene	Unknown		Unknown	
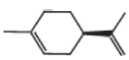	*R*-(+)-limonene	Unknown		Unknown	

[a] α-phellandrene, β-pinene, γ-terpinene, and terpinolene were also assayed and determined to not be substrates.

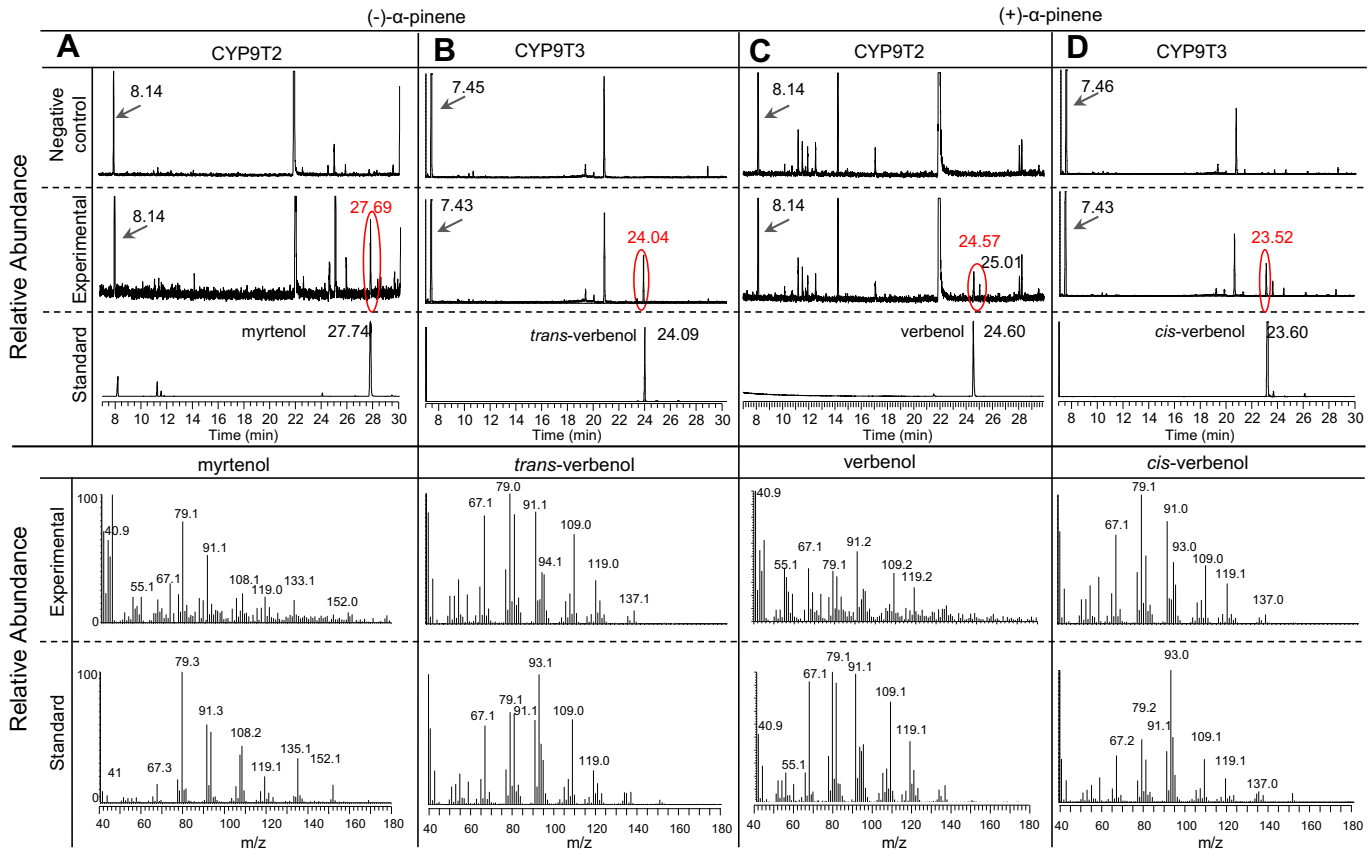

Fig. 4. α-Pinene hydroxylation. Gas chromatograph traces with single ion monitoring at $m/z = 79$ (above) and mass spectra (below) of extracts of *in vitro* incubations of (+)-α-pinene (**A**, **B**) or (−)-α-pinene (**C**, **D**) with Sf9 cell microsomes bearing recombinant *CYP9T2*, *CYP9T3* or cytochrome P450 reductase (control). GC profiles and mass spectra of authentic standards are also shown. Substrates are noted by an arrow and products by a red oval. The 24.57 min and 25.01 min peaks in (**C**) correspond to *trans*- and *cis*-verbenol, respectively. Mass spectra are of circled products or authentic standards. (For interpretation of the references to colour in this figure legend, the reader is referred to the web version of this article.)

bark beetle pheromone evolution and constraints affecting cytochrome P450 activity.

The 94% a.a. identity between *CYP9T2* and *CYP9T3* suggests their genes are allelic, though we cannot discard the possibility that they are paralogous. *CYP9T2* is considered pheromone-biosynthetic in part because it is coordinately regulated with other pheromone-biosynthetic genes, including *GPPS/MS*), which encodes the enzyme catalyzing myrcene biosynthesis (Blomquist et al., 2010;

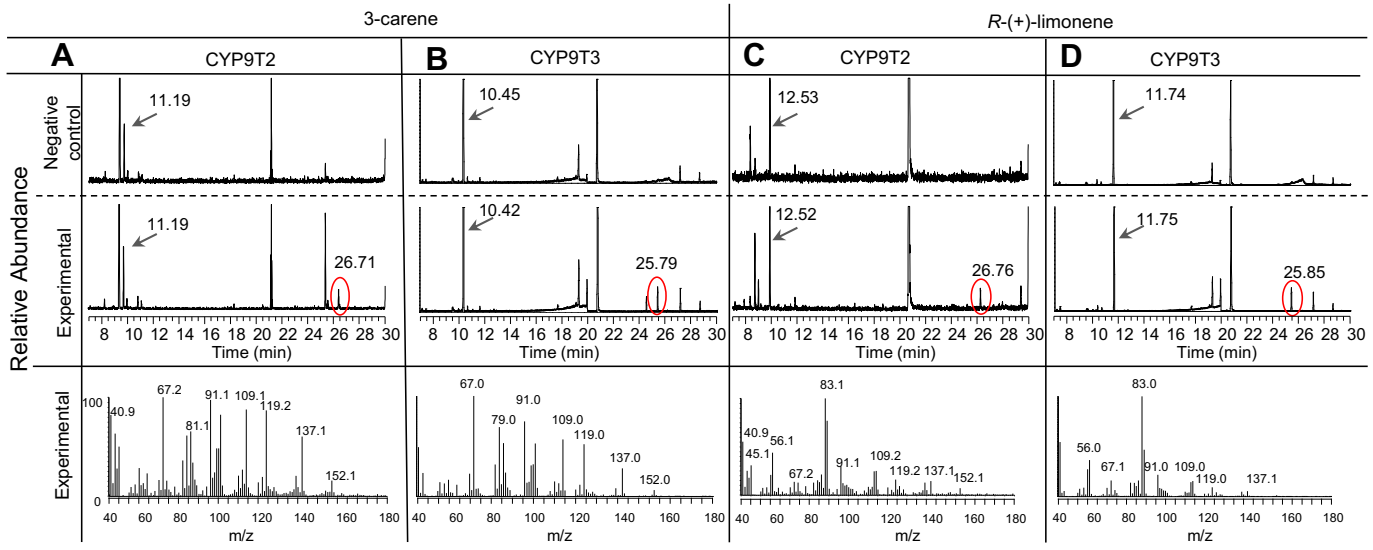

Fig. 5. Hydroxylation of 3-carene and *R*-(+)-limonene. Gas chromatograph traces with single ion monitoring at $m/z = 79$ (above) and mass spectra (below) of extracts of *in vitro* incubations of 3-carene (**A**, **B**) or *R*-(+)-limonene (**C**, **D**) with Sf9 cell microsomes bearing recombinant *CYP9T2*, *CYP9T3*, or cytochrome P450 reductase (control). Substrates are noted by an arrow and products by a red oval. The 21.96 min peak corresponds to the internal standard, *n*-octanol. (**C, D**) Mass spectra are of circled products. Products from reactions with 3-carene and *R*-(+)-limonene could not be confidently identified.

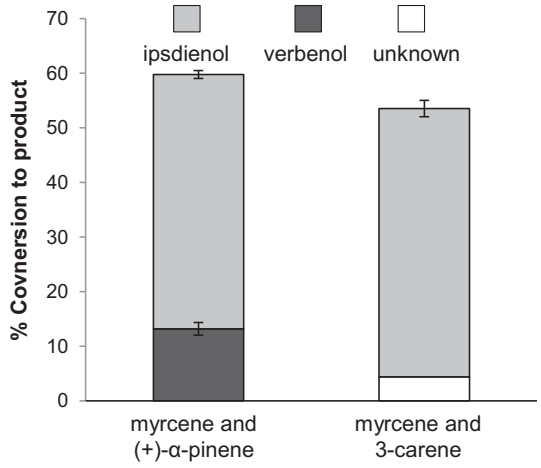

Fig. 6. *CYP9T2* substrate preference assay. Sf9 cell microsomes containing recombinant *CYP9T2* and CPR were incubated together for 3 h in the presence of both myrcene and (+)-α-pinene or myrcene and 3-carene. Following extraction and GC analysis, the relative amounts of observed products were determined from peak areas. Values are means of three replicates ± std. err.

Gilg et al., 2009). Indeed, the observed lack of induction by myrcene of *CYP9T2* mRNA parallels the non-response of *GPPS/MS* (Fig. 2). CYP9T1, which also has 94% a.a. identity to *CYP9T2*, is a pheromone-biosynthetic myrcene hydroxylase from *I. confusus* (Sandstrom et al., 2008). *CYP9T1*, *CYP9T2*, and *GPPS/MS* are regulated by juvenile hormone (JH) III (Blomquist et al., 2010). While the expression profile and regulation of *CYP9T3* have not been determined, its very similar substrate and product profile and high sequence identity compared to *CYP9T2* suggest each performs a similar role in their respective populations. Thus, *CYP9T3* is likely important for pheromone biosynthesis in eastern *I. pini*.

CYP9T2 and *CYP9T3* hydroxylated myrcene in the same position and with extreme specificity; other possible hydroxylation products such as amitinol or myrcenol were never observed. However, they differed in the enantiomeric ratios of ipsdienol they produced (Fig. 3). Our observation that CYYP9T2 produced an approximate 80:20 ratio of (−)-:(+)-ipsdienol confirms that of Sandstrom et al. (2006). The ~90:10 ratio produced by *CYP9T3* in this study was statistically different from the ratio produced by *CYP9T2* (Fig. 3). The different enantiomeric ratios are unlikely to be biologically relevant as downstream enzymes such as ipsdienol dehydrogenase (IDOLDH) likely change them (Figueroa-Teran et al., 2012). However, this information can provide insight into structure–function relationships for these enzymes. The greater percentage of (4*R*)-(−)-ipsdienol produced by *CYP9T3* might be caused by slight differences in the solvent access channel that restricts the substrate's approach to the active site (Bernhardt, 2006; Li et al., 2004) such that myrcene is oriented with the (4*R*)-(−) pro-chiral hydrogen in a position to be hydroxylated slightly more often than the (4*S*)-(+) pro-chiral hydrogen. Such differences are likely due to amino acid changes either in the substrate binding site or solvent channel, or at secondary sites that affect the overall tertiary structure. Small changes at secondary sites can significantly affect substrate and/or product range (Bernhardt, 2006; Li et al., 2004). For example, single amino acid substitutions outside the active site of CYP2B4 translated into large effects on substrate catalysis and enzyme inhibition (Wilderman et al., 2011).

Such changes may also explain the different product profiles from α-pinene (Fig. 4). *CYP9T3* produced *cis*-verbenol and *trans*-verbenol from (+)-α-pinene and (−)-α-pinene, respectively. The small differences in the retention times between standards and identifiable peaks are likely the result of the samples and standards often being analyzed on separate days; larger differences in standard and product elution times for the two enzymes is similarly likely due to the assays for each being performed months apart (Figs. 4 and 5). It is most interesting that *CYP9T2* and *CYP9T3* produced myrtenol and (−)-*trans*-verbenol, respectively, from (−)-α-pinene (Fig. 4). A strict bias in terms of location and orientation of the hydroxylation was also apparent for *CYP9T2* and *CYP9T3* when given 3-carene or (+)-limonene as substrates (Fig. 5). The extreme region-specificity of the hydroxylation reinforces the significance of modest structural changes in determining P450 activity. Insight into the structure–function relationship can be gained in the future by combining these functional data with multiple homology models of closely related P450s (Bernhardt, 2006; Li et al., 2004).

The relatively broad substrate range for *CYP9T2* and *CYP9T3* raises a question of the extent to which they favor a particular monoterpene. A clear answer requires kinetic data (K_m and V_{max} values) that are difficult to accurately measure given the volatility of the products. Nonetheless, our competition experiments suggest that *CYP9T2* greatly prefers myrcene over (α)-pinene and 3-carene (Fig. 6). This preference is consistent with the primary role of *CYP9T2* in converting myrcene to pheromone. The lack of *CYP9T2* induction by its preferred substrate, myrcene, underscores its tight regulation by JH III. If the paradigm that pheromone production evolved from resin detoxification is accurate (Byers and Birgersson, 2012; Hughes, 1974), it is tempting to speculate that tight endocrine regulation coupled with a preference for myrcene indicates pressure to channel *CYP9T2* (and probably *CYP9T3*) activity toward pheromone biosynthesis. Indeed, coordinate regulation of *CYP9T2* and *GPPS/MS* suggests strong pressure for *CYP9T2* to clear myrcene produced *de novo* by GPPS/MS. The ability to accept other resin monoterpenes thus may indicate a presumed broader substrate range for a resin-detoxifying ancestral enzyme. However, there are very few examples where functional assays support an inferred metabolic role derived from expression data for an insect P450 (Li et al., 2004). More bark beetle monoterpene hydroxylating P450s need to be identified and characterized in order to clarify the evolutionary link between resin detoxification and pheromone biosynthesis in pine bark beetles.

Acknowledgments

We thank the Whittell Board for permission to collect beetle-infested logs from the UNR Little Valley forest, members of CT's, MDG's and GJB's laboratories for collecting beetles, and the Nevada Proteomics Center for GC–MS analyses. We are grateful to anonymous reviewers for suggestions that significantly strengthened the manuscript. This work was supported by the USDA (2006-35604-16727, 2009-05200), NSF (IOS-0642182), and the Nevada Agricultural Experiment Station (NEV00374).

Appendix A. Supplementary data

Supplementary data related to this article can be found at http://dx.doi.org/10.1016/j.ibmb.2013.01.003.

References

Altschul, S.F., Gish, W., Miller, W., Myers, E.W., Lipman, D.J., 1990. Basic local alignment search tool. Journal of Molecular Biology 215, 403–410.
Bernhardt, R., 2006. Cytochromes P450 as versatile biocatalysts. Journal of Biotechnology 124, 128–145.
Blomquist, G.J., Figueroa-Teran, R., Aw, M., Song, M., Gorzalski, A., Abbott, N.L., Chang, E., Tittiger, C., 2010. Pheromone production in bark beetles. Insect Biochemistry and Molecular Biology 40, 699–712.
Browne, L.E., 1972. An emergence cage and refrigerated collector for wood-boring insects and their associates. Journal of Economic Entomology 65, 1499–1501.

Byers, J.A., Birgersson, G., 2012. host-tree monoterpenes and biosynthesis of aggregation pheromones in the bark beetle *Ips paraconfusus*. Psyche. http://dx.doi.org/10.1155/2012/539624.

Choi, S., Kim, M., Kim, S.I., Jeon, J.K., 2003. Microplate assay measurement of cytochrome P450-carbon monoxide complexes. Journal of Biochemistry and Molecular Biology 36, 332–335.

Domingue, M., Starmer, W., Teale, S., 2006. Genetic control of the enantiomeric composition of ipsdienol in the pine engraver, *Ips pini*. Journal of Chemical Ecology 32, 1005–1026.

Domingue, M., Teale, S., 2008. The genetic architecture of pheromone production between populations distant from the hybrid zone of the pine engraver, *Ips pini*. Chemoecology 17, 255–262.

Feyereisen, R., 2005. Insect Cytochromes P450. In: Gilbert, L.I., Iatrou, K., Gill, S.S. (Eds.), Comprehensive Molecular Insect Science. Elsevier BV, pp. 1–77.

Figueroa-Teran, R., Welch, W.H., Blomquist, G.J., Tittiger, C., 2012. Ipsdienol dehydrogenase (IDOLDH): a novel oxidoreductase important for *Ips pini* pheromone production. Insect Biochemistry and Molecular Biology 42, 81–90.

Gilg, A.B., Bearfield, J.C., Tittiger, C., Welch, W.H., Blomquist, G.J., 2005. Isolation and functional expression of the first animal geranyl diphosphate synthase and its role in bark beetle pheromone biosynthesis. Proceedings of the National Academy of Sciences of the United States of America 102, 9760–9765.

Gilg, A.B., Tittiger, C., Blomquist, G.J., 2009. Unique animal prenyltransferase with monoterpene synthase activity. Naturwissenschaften 96, 731–735.

Hager, B.J., Teale, S.A., 1996. The genetic control of pheromone production and response in the pine engraver beetle *Ips pini*. Heredity 77, 100–107.

Hellemans, J., Mortier, G., De Paepe, A., Speleman, F., Vandesompele, J., 2007. qBase relative quantification framework and software for management and automated analysis of real-time quantitative PCR data. Genome Biology 8, R19.

Huber, D.P., Erickson, M.L., Leutenegger, C.M., Bohlmann, J., Seybold, S.J., 2007. Isolation and extreme sex-specific expression of cytochrome P450 genes in the bark beetle, *Ips paraconfusus*, following feeding on the phloem of host ponderosa pine, Pinus ponderosa. Insect Molecular Biology 16, 335–349.

Hughes, P.R., 1974. Myrcene: a precursor of pheromones in *Ips* beetles. Journal of Insect Physiology 20, 1274–1275.

Keeling, C.I., Bearfield, J.C., Young, S., Blomquist, G.J., Tittiger, C., 2006. Effects of juvenile hormone on gene expression in the pheromone-producing midgut of the pine engraver beetle, *Ips pini*. Insect Molecular Biology 15, 207–216.

Li, W., Schuler, M.A., Berenbaum, M.R., 2003. Diversification of furanocoumarin-metabolizing cytochrome P450 monooxygenases in two papilionids: specificity and substrate encounter rate. Proceedings of the National Academy of Sciences of the United States of America 100, 14593–14598.

Li, X., Baudry, J., Berenbaum, M.R., Schuler, M.A., 2004. Structural and functional divergence of insect CYP6B proteins: from specialist to generalist cytochrome P450. Proceedings of the National Academy of Sciences of the United States of America 101, 2939–2944.

Mao, W., Rupasinghe, S., Zangerl, A.R., Schuler, M.A., Berenbaum, M.R., 2006. Remarkable substrate-specificity of CYP6AB3 in *Depressaria pastinacella*, a highly specialized caterpillar. Insect Molecular Biology 15, 169–179.

Omura, S., Sato, R., 1964. The carbon monoxide-binding pigment of liver microsomes II. Journal of Biological Chemistry 239, 2379–2385.

Sandstrom, P., Ginzel, M.D., Bearfield, J.C., Welch, W.H., Blomquist, G.J., Tittiger, C., 2008. Myrcene hydroxylases do not determine enantiomeric composition of pheromonal ipsdienol in *Ips* spp. Journal of Chemical Ecology 34, 1584–1592.

Sandstrom, P., Welch, W.H., Blomquist, G.J., Tittiger, C., 2006. Functional expression of a bark beetle cytochrome P450 that hydroxylates myrcene to ipsdienol. Insect Biochemistry and Molecular Biology 36, 835–845.

Shumate, A., Teale, S., Ayres, B., Ayres, M., 2011. Disruptive selection maintains variable pheromone blends om the bark beetle *Ips pini*. Environmental Entomology 40, 1530–1540.

Wen, Z., Pan, L., Berenbaum, M.R., Schuler, M.A., 2003. Metabolism of linear and angular furanocoumarins by Papilio polyxenes CYP6B1 co-expressed with NADPH cytochrome P450 reductase. Insect Biochemistry and Molecular Biology 33, 937–947.

Wilderman, P.R., Gay, S.C., Jang, H.-H., Zhang, Q., Stout, C.D., Halpert, J.R., 2011. Investigation by site-directed mutagenesis of the role of cytochrome P450 2B4 non-active site residues in protein-ligand interactions based on crystal structures of the ligand-bound enzyme. FEBS Journal, 1607–1620.